Ag$_{11}$(SG)$_7$: A New Cluster Identified by Mass Spectrometry and Optical Spectroscopy

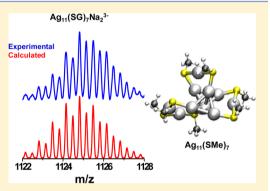Ananya Baksi,[†,§] M. S. Bootharaju,[†,§] Xi Chen,[‡] H. Häkkinen,[‡] and T. Pradeep*[,†]

[†]DST Unit of Nanoscience (DST UNS), and Thematic Unit of Excellence (TUE), Department of Chemistry, Indian Institute of Technology Madras, Chennai 600 036, India

[‡]Departments of Chemistry and Physics, Nanoscience Center, University of Jyväskylä, FI-40014 Jyväskylä, Finland

Ⓢ *Supporting Information*

ABSTRACT: We report a one-step and high yield synthesis of a red-luminescent silver cluster with the molecular formula, Ag$_{11}$(SG)$_7$ (SG: glutathionate) via reduction of silver ions by sodium borohydride in the presence of the tripeptide, glutathione (GSH). The as-prepared cluster shows prominent absorption features at 485 and 625 nm in its UV–vis absorption spectrum. Aging of the as-prepared cluster solution led to the disappearance of the 625 nm peak, followed by broadening of the 485 nm peak to give three maxima at ~487, 437, and 393 nm in its absorption spectrum. These peaks remain unchanged even after polyacrylamide gel electrophoresis (PAGE), where a single band was observed confirming high purity of the cluster formed. Electrospray ionization mass spectrometry (ESI MS) reveal the composition of the cluster to be Ag$_{11}$(SG)$_7$ with multiple sodium attachments to the ligand to give −3 and −2 charged species. These compositions match well with their calculated isotope patterns. Extensive MS/MS was performed to understand the fragmentation. Potential atomic structures are discussed based on density functional theory calculations and comparisons for optical absorption spectra using Ag$_{11}$(SCH$_3$)$_7$ as the model. Photoluminescence of this cluster was selectively quenched in the presence of Hg(II) and Cu(II) separately. Detection limit was found to be below their permissible limits in drinking water set by US EPA. Ag$_{11}$(SR)$_7$ cluster is reported for the first time.

INTRODUCTION

Exploration of atomically precise monolayer-protected clusters of metals, particularly those of Au,[1−4] Ag,[5,6] Cu,[7] Pt,[8] and Pd,[9] is progressing enormously in the past decade due to interest in their unique optical, chemical, and biological properties. A series of gold and silver clusters with monolayer protection have been synthesized by several means, although synthesis of these clusters with atomic precision and their thorough characterization to obtain exact molecular formulas are challenging. The most common and well-established synthetic route is the reduction of an appropriate metal precursor in the presence of ligands of choice (water- or organic-soluble)[10,11] under suitable experimental conditions. Some of the other routes are core and interfacial etching of nanoparticles,[12] galvanic exchange,[13] microwave irradiation,[14] reduction by CO,[15] solid state route,[16−18] sonochemical,[19] and sunlight-mediated[20] methods. Protein- and polymer-coated silver and gold nanoclusters have also been prepared.[21] Cavities within gels were used to control the growth of clusters.[22]

The most difficult task in characterization of clusters is finding their molecular formulas. Many reports are limited to the synthesis and studies of optical properties. The most reliable way to obtain the molecular formula of the clusters is from their crystal structures. Several crystal structures of noble metal nanoclusters exist although a large number of clusters are awaiting crystallization. A good number of thiol-protected gold clusters, namely, Au$_{25}$(SR)$_{18}$,[23,24] Au$_{36}$(SR)$_{24}$,[25] Au$_{38}$(SR)$_{24}$,[26] Au$_{102}$(SR)$_{44}$,[27] Au$_{30}$S(SR)$_{18}$,[28] etc., have been crystallized due to their better stability. However, inherently poor stability limited the crystallization of silver clusters to just a few; namely, [Ag$_{14}$(SC$_6$H$_3$F$_2$)$_{12}$(PPh$_3$)$_8$],[29] [Ag$_{16}$(DPPE)$_4$(SC$_6$H$_3$F$_2$)$_{14}$],[30] [Ag$_{32}$(DPPE)$_5$(SC$_6$H$_4$CF$_3$)$_{24}$],[30] and [Ag$_{44}$(SR)$_{30}$].[31,32] Apart from the crystal structure, mass spectrometry is another way to understand the molecular formulas of the clusters.[33−38] There are many reports of mass spectrometric studies of monolayer-protected gold clusters, but the number is still limited in the case of silver clusters especially when they are water-soluble. There are reports on silver clusters such as Ag$_7$(DMSA)$_4$,[39] Ag$_{7,8}$(MSA)$_{7,8}$,[12] Ag$_9$(MSA)$_7$,[17] Ag$_9$(SG)$_6$,[40] Ag$_{15}$(SG)$_{11}$,[41] Ag$_{16}$(SG)$_9$,[40] Ag$_{31}$(SG)$_{19}$,[41] Ag$_{32}$(SG)$_{19}$,[41,42] Ag$_{44}$(SR)$_{30}$,[43,44] Ag$_{75}$(SG)$_{40}$,[45] Ag$_{152}$(PET)$_{60}$,[18] etc., whose chemical formulas were obtained using mass spectrometry (DMSA, MSA, SG, and PET refer to dimercaptosuccinic acid, mercaptosuccinic acid, glutathione and phenylethanethiol, all in the thiolate form).

With regard to applications of noble metal clusters, there are reports on their use in energy, environment, biology, catalysis,

etc.[46] One of the important advantages of water-soluble clusters is their use in sensing toxic metal ions in drinking water. Metal ions such as mercury, cadmium, and lead cause severe health effects in human and aquatic life.[16] It is very important to develop sensors for selective detection of this kind of ions down to their permissible levels. Absorption and photoluminescence features are found to be affected by the interactions of metal ions (and anions) with clusters. Possible reasons for photoluminescence quenching are aggregation of clusters,[47] redox reactions,[16] metallophilic interactions,[13] etching,[48] etc.

In this article, we report a one-step and high yield synthesis of monodispersed red-luminescent silver cluster of composition $Ag_{11}(SG)_7$. This core is reported for the first time. This cluster is characterized using mass spectrometric (ESI MS), spectroscopic (UV−vis absorbance, photoluminescence, X-ray photoelectron, and infrared spectroscopy), and microscopic (transmission electron microscopy) tools. Computational modeling suggests a structural motif that is validated by the comparison of calculated and measured optical absorption spectra. These clusters were employed for sensing Hg(II) and Cu(II) in water.

■ EXPERIMENTAL SECTION

Chemicals. All the chemicals were procured from various sources and used without further purification. Silver nitrate ($AgNO_3$, 99%), glutathione reduced (GSH, 97%, Aldrich), acrylamide (AR grade), N,N^I-methylenebis(acrylamide) (BIS) (AR grade), ammonium persulfate, and N,N,N^I,N^I-tetramethylethylene diamine (TEMED) were obtained from SRL Chemical Co. Ltd., India. Sodium borohydride ($NaBH_4$, 99.99%, Aldrich), ethanol (HPLC grade, 99.9%, Aldrich), and methanol (HPLC grade) were used as received.

Synthesis of $Ag_{11}(SG)_7$. About 650 mmol of GSH was added to 50 mL of MeOH under ice cold conditions maintained through ice bath and stirred for 10 min. About 130 mmol of $AgNO_3$, dissolved in 0.5 mL of Millipore water was mixed with the GSH solution, and the mixture was stirred for 15 min to form silver thiolates. About 7 mL (1.4 mol) of ice cold sodium borohydride was added to the mixture dropwise, and the solution stirred for another 15 min for complete reduction of thiolates to clusters. The as-formed clusters were not completely soluble in methanol, and they started precipitating. Excess MeOH was added for complete precipitation. The sample was centrifuged at 7000 rpm and washed repeatedly with methanol to remove the excess ligand and thiolates. The precipitate was dried by rotavapor evaporation to get a powder. About 55 mg of powder can be achieved in a single synthesis, and hence, the yield is about 85% in terms of Ag content in the reactant and the product.

Polyacrylamide Gel Electrophoresis (PAGE). PAGE was performed as per the literature.[17] A Biorad, Mini-protein Tetra cell with 1 mm thick spacer was utilized to process the PAGE. The as-prepared cluster was dissolved in water (10 mg/mL) and kept at 20 °C for 30 min. After that, the solution was centrifuged at 5000 rpm for 3−4 min and dissolved in 5% (v/v) glycerol−water solution (1 mL). The sample solution (1 mL) was loaded onto a 1 mm gel and eluted for 5 h at a constant voltage of 150 V. Only a single band was observed. The gel fraction containing the clusters was cut out, and the cluster was extracted into distilled water. The extracted cluster solution was centrifuged to remove the gel material and used further for UV−vis, PL, and ESI MS study.

Sensing Metal Ions. Solutions of the cluster (∼1 mg/mL water) and metal ions of known concentration were prepared

initially. Equal volumes of cluster and metal ion solutions (typically 3 mL each) were mixed, and PL measurements were taken after 5 min. It should be noted that the concentrations of metal ions mentioned are the final values in these solutions.

Instrumentation. UV−vis spectra were recorded with a PerkinElmer Lambda 25 instrument in the range of 200−1100 nm with a band-pass of 1 nm. Photoluminescence measurements were carried out on a Jobin Yvon NanoLog instrument. The band-pass for excitation and emission was set at 3 nm. X-ray photoelectron spectroscopy (XPS) measurements were done using an Omicron ESCA Probe spectrometer with polychromatic Mg K_α X-rays ($h\nu$ = 1253.6 eV) with a constant analyzer energy of 20 eV. High resolution transmission electron microscopy of clusters was carried out with a JEOL 3010 instrument. The samples were drop-cast on carbon-coated copper grids and allowed to dry under ambient conditions. FTIR spectra were measured with a PerkinElmer Spectrum One instrument. KBr crystals were used as the matrix for preparing samples.

Mass Spectrometric Analysis. Thermo scientific LTQ XL ESI MS was used for mass spectrometric analysis. Experiments were carried out in both positive and negative ion modes, but nothing significant was observed in the positive mode other than the ligand. Therefore, further experiments were done in the negative ion mode. MS^2 experiments were performed in the collision induced dissociation (CID) mode with varying collision energy. We have also performed a capillary temperature-dependent study, but no extra peak was observed. As the instrumental settings are important, we list them below:

solvent: 1:1 (v/v) H_2O/MeOH
sample flow rate: 10 μL/min
vaporizer temperature: 582 °C
capillary temperature: 275 °C
source voltage: 5.47 kV
source current: −6.31 μA
capillary voltage: −42.97 V
tube lens voltage: −82.66 V

We have performed several control experiments to confirm that our cluster is not a fragment from a bigger cluster due to the temperature or potentials used in ESI MS. We have performed a capillary temperature-dependent experiment ranging from 80 to 300 °C, and no change in the mass spectrum was seen. We have also changed source voltage from 1.5 kV to 8 kV and found that only peak intensity changes while changing the voltage. No new peak appeared at higher mass at lower voltages or reduced temperatures.

■ RESULTS AND DISCUSSION

Spectroscopic Characterization. Clusters were synthesized following the above-mentioned method. The reaction was done in the presence of excess MeOH at ice cold conditions. MeOH was used for precipitating the clusters and to remove excess ligand and thiolate, which probably helped us to get this stable cluster in solution. In our method, we have done the reaction in MeOH, and hence, once the cluster was formed, it started precipitating due to the presence of excess MeOH in the solution. By this process we could avoid contamination of excess ligand and thiolates, which are soluble in methanol. The precipitate was centrifuged and washed repeatedly to remove excess thiol (if any) and dried by rotavapor to get a powder. The yield was 85% in terms of the silver content.
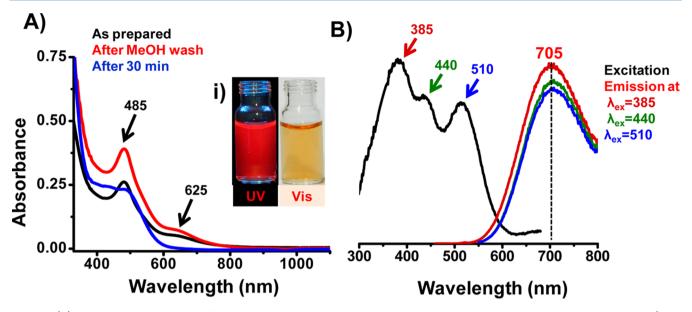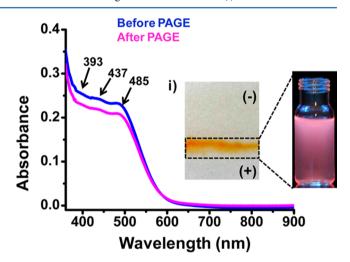
Figure 1. (A) UV–vis absorption spectra of as-synthesized, washed, and aged silver cluster. The clusters show two peaks at 485 and 625 nm (black and red traces) where the 625 nm peak disappeared with time and the other peak broadened into three smaller humps positioned at 393, 437, and 487 nm (blue trace). Photoluminescence spectra are shown in B, where all the three excitation maxima (385, 440, and 510 nm) resulted in a single emission maximum at 705 nm. Photographs of the as-synthesized cluster under UV and visible light are shown in inset (i).

Optical absorption spectrum of the as-synthesized (crude, without washing) cluster showed two humps positioned at 625 nm (1.98 eV) and 485 nm (2.55 eV), with the latter being more prominent. The peak positions remain the same after washing with MeOH. The peak shape started changing with the disappearance of the 625 nm peak and broadening of the 485 nm peak, which resulted in three relatively smaller humps centered at 487, 437, and 393 nm. This happened at room temperature (25 °C) when the clusters were dissolved in water and kept for 30 min (see Figure 1A). This conversion implies that in the beginning a metastable cluster was formed, which was converted to a stable one in solution. After this, the spectrum remained the same without any change in absorbance.

Three distinct excitation peaks were observed at 385, 440, and 510 nm in the photoluminescence spectrum, all of which resulted in the same emission maximum at 705 nm (Figure 1B). The clusters are red-luminescent under UV irradiation as shown in Figure 1A. As reported before, water-soluble silver clusters do not show high quantum yield unlike gold clusters. We have obtained a quantum yield of 0.8% for these clusters using Rhodamine 6G as the reference.

To check whether the cluster is a single one or a mixture, we have performed PAGE separation, a well developed technique in cluster science. We have observed a single band in PAGE (see the inset of Figure 2) confirming the high purity of the as-synthesized cluster. There are reports[49] where PAGE was used for the analysis of mixture of clusters.

We have cut the band, and the cluster was extracted into water for further study. The same UV–vis absorption features were observed confirming that the cluster is monodisperse in as-synthesized form (Figure 2). The band was also fluorescent under UV irradiation and showed similar excitation and emission feature in the photoluminescence spectra as shown in Figure 1B. We have compared our UV–vis absorption data with previously reported glutathione protected silver clusters.[49] Our absorption spectral data are nearly matching with band 2 in this report, which was assigned to be Ag$_{15}$. This implies our cluster is unlikely to be bigger than Ag$_{15}$. Monodisperse clusters
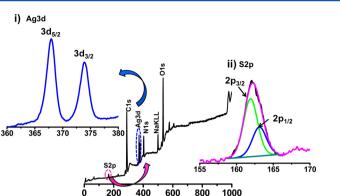

Figure 2. UV–vis absorption spectra of silver clusters remain the same before and after PAGE separation. A single band in PAGE (inset (i)) confirms the high purity of the cluster in the as-synthesized form. The band was cut and the cluster was extracted into water. This cluster exhibits red luminescence under UV irradiation (shown on the right).

were observed in TEM analysis with an average size of 1 nm as shown in Figure S1 (Supporting Information). XPS survey spectrum of clusters confirms the presence of elements, Ag, S, C, O, N, and Na (Figure 3). Silver in the cluster close to the zerovalent state was confirmed from the Ag 3d$_{5/2}$ position in XPS (368.0 eV) (Figure 3i). However, the S 2p$_{3/2}$ peak at 162.5 eV proved the Ag–S bonding in the cluster (Figure 3ii). Thiolate bound to noble metals is seen at this binding energy (BE).[12] Infrared spectroscopy was performed to check the corresponding changes in the ligand after cluster formation. The S–H stretching frequency at 2525 cm^{-1} was absent after cluster formation, which confirms successful binding of Ag to sulfur of glutathione (Figure S2, Supporting Information).

Mass Spectrometric Understanding. A 1:1 MeOH:H$_2$O (v/v) mixture was used for further characterization of the

Figure 3. XPS survey spectrum of AgSG cluster showing all the expected elements, Ag, S, C, O, N, and Na. Ag 3d and S 2p regions are expanded in (i) and (ii), respectively, showing Ag in Ag^0 state and sulfur bound to metal.

cluster using ESI MS. A negative ion ESI MS is shown in Figure 4 where two distinct envelopes (labeled *) were observed in
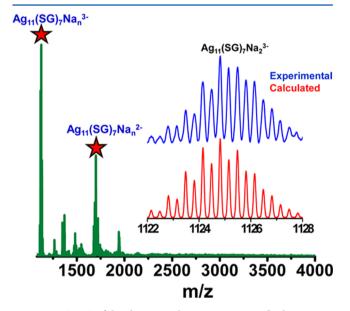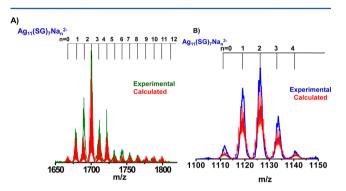

Figure 4. ESI MS of the clusters in the negative ion mode showing −2 and −3 charged species along with some thiolates. Main peaks are marked with the * symbol. Experimental spectrum (blue trace) is in good agreement with the calculated mass spectrum (red trace) of the species as shown in the inset.

the mass range of m/z 1100−1200 and 1650−1800 with specific separation between the neighboring peaks due to sodium attachment. Besides, a few thiolates were also seen. The optimized conditions are given in the experimental section. No peak was observed in the higher mass region confirming absence of any bigger cluster core. We have thoroughly examined each and every parameter affecting the mass spectrum. We have performed flow rate, capillary voltage, and capillary temperature dependence in details. At lower flow rate, peaks were not resolved well with proper isotope distribution. At higher flow rate, peaks become broader. About 10 μL/min was the optimum flow rate where we achieved a good signal intensity as well as resolution. We have tried to see the effect of capillary temperature over a range of 80 to 300 °C with 10 °C increase in each step. Here, no difference in the peak positions

other than signal intensity was noticed. As the cluster is smaller in size, it might be a fragment from a bigger parent cluster, which can happen in the presence of high voltage. We did not find any new peak at lower (1.5 kV) as well as higher (8 kV) source voltages, confirming that this is a new cluster and not a fragment. Note that smaller clusters like Ag_7, Ag_8, Ag_9, etc., were reported and characterized before, using ESI MS.[12,16,17] We also have checked ESI MS of the PAGE separated sample, which resulted in the same mass peaks. Experimental and calculated spectra are in agreement with the assigned species as shown in the inset of Figure 4 for a triply charged species.

Peaks in the m/z 1100−1200 region are separated by m/z 7.3 corresponding to a triply charged species (Figure 5A),
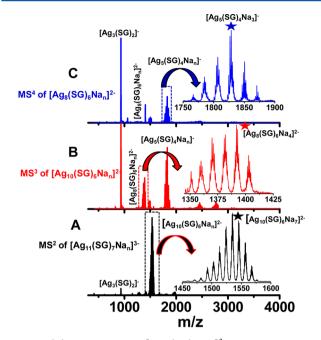

Figure 5. Expanded negative mode ESI MS of $Ag_{11}(SG)_7$ clusters in m/z 1100−1150 (A) and 1650−1800 (B) ranges. Multiple sodium attachments to glutathione ligand is evident from both the double (A) and triply (B) charged species. Good match of the experimental and calculated mass spectra for $Ag_{11}(SG)_7$ with and without sodium adducts is also seen.

suggesting the presence of a species with Na attachment (m/z [Na−H]/3 = 7.33), whereas the separation is m/z 11 (m/z [Na−H]/2 = 11) for doubly charged species (in the range of m/z 1650−1800, Figure 5B). On the basis of these, the cluster is assigned to have a formula $Ag_{11}(SG)_7$.

Analogous Au clusters have been reported as well as crystallized with phosphine ligand in 1970.[4,50] The calculated mass spectra of the clusters with specific charge state matches well with the experimentally observed one as shown in the inset of Figure 5A,B where both triply charged and doubly charged envelopes are expanded and plotted along with the calculated spectra. Multiple Na attachments are possible with GSH due to the presence of two −COOH groups. Such attachments were observed in Ag clusters before.[12,16,17] For this specific cluster of interest, which contains 7 ligands, a maximum of 13, 12, and 11 Na attachments are possible for singly, doubly, and triply negative species, respectively. This observation was clear for the −2 charge region where a series of peaks separated by m/z 11 were observed and a maximum of 12 Na attachments is clear confirming the exact number of ligands (Figure 5B).

Extensive MS/MS analysis was performed to understand the fragmentation pattern of the ions (Figure 6). When the triply charged species (m/z 1130 was selected with an isotope width of 60, i.e., m/z 1100−1160, assigned to $Ag_{11}(SG)_7Na_n^{3-}$) was allowed to fragment under collision induced dissociation (CID) with varying collision energy (Figure S3, Supporting Information), it readily loses one AgSG and forms $Ag_{10}(SG)_6^{2-}$. At higher collision energy, we can also see some smaller thiolate fragments such as $Ag_3SG_2^-$. When this $Ag_{10}(SG)_6^{2-}$ fragment was further allowed to dissociate under
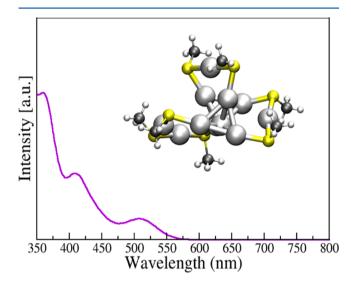
Figure 6. (A) ESI MS/MS of $[Ag_{11}(SG)_7Na_n]^{3-}$ showing one AgSG loss, and the corresponding peak is $[Ag_{10}(SG)_6Na_n]^{2-}$. Collision energy dependence study of $Ag_{11}(SG)_7Na_n^{3-}$ is shown in Figure S5, Supporting Information. When $[Ag_{10}(SG)_6Na_n]^{2-}$ fragment was further dissociated in MS^3, it fragments to various thiolates like $Ag_3(SG)_2^-$, $Ag_5(SG)_4^-$, $Ag_8(SG)_6^-$, etc., as shown in B. Same fragments were also observed with $Ag_8(SG)_6Na_n^{2-}$ alone under MS^4 to produce $Ag_5(SG)_4Na_n^-$ and $Ag_3(SG)_2^-$ as shown in C.

CID (MS^3), it leads to various thiolates namely, $[Ag_3(SG)_2]^-$ (m/z 935), $[Ag_8(SG)_6Na_n]^{2-}$ (m/z 1349 for n = 0), $[Ag_5(SG)_3Na_n]^-$ (m/z 1457 for n = 0), $[Ag_5(SG)_4Na_n]^-$ (m/z 1763 for n = 0), and $[Ag_7(SG)_6Na_n]^-$ (m/z 2591 for n = 0) (Figure 6B). Further fragmentation of $[Ag_8(SG)_6Na_n]^{2-}$ led to $[Ag_3(SG)_2]^-$ and $[Ag_5(SG)_4Na_n]^-$ fragments (Figure 6C). MS/MS of doubly charged species resulted in one AgSG loss similar to the triply charged one (Figure S4, Supporting Information). Some species of higher masses were also observed when higher collision energies were used. These species include $[Ag_{12}(SG)_{10}Na_n]^{2-}$ (m/z 2177 for n = 0) and $[Ag_{16}(SG)_{15}Na_n]^{3-}$ (m/z 2105 for n = 0) along with other thiolates. This phenomenon can be explained in terms of gas phase association of the fragments in the trap to form larger thiolates. If we look at the fragments carefully, most of them consist of at least one extra metal atom compared to the ligand. Considering a linear chain of thiolates, the Ag atoms in them may be positioned at the tail of the chain, and they may associate with other fragments of free ligands (generated by CID).

This in fact proves the accessibility of reacting molecules to the Ag sites in the cluster. This observation proposes new possibilities for catalysis and gas phase reactions. Single cluster (by trapping specific ion) catalysis may be achieved for reactions such as oxidation of CO and alkene to CO_2 and epoxide, respectively. Note that such types of catalysis are reported for gas phase gold and silver clusters.[51−53] $Au_{25}(SR)_{18}$ and $Au_{38}(SR)_{24}$ were used successfully as a catalyst for the conversion of CO to CO_2 where a metal oxide, CeO_2, was used as the support.[54−56]

Theoretical Calculation. Structural search via density functional theory (DFT) by using $Ag_{11}(SCH_3)_7$ as a model

system indicated a family of low-energy structures that all share an Ag_7 core protected with two $Ag(SR)_2$ and one $Ag_2(SR)_3$ motifs. Figure S5, Supporting Information, shows six structural candidates that are all located within 0.85 eV (Table S1, Supporting Information). Their HOMO−LUMO energy gaps vary within 1.65 to 2.29 eV indicating a remarkable electronic stability. The computed optical spectra show two to three absorption features (Figure S6a−f, Supporting Information). The best agreement to experiment is shown by structure "**f**" that has absorption maxima 360, 410, and 509 nm as shown in Figure 7. These compare quite well to the experimental peaks
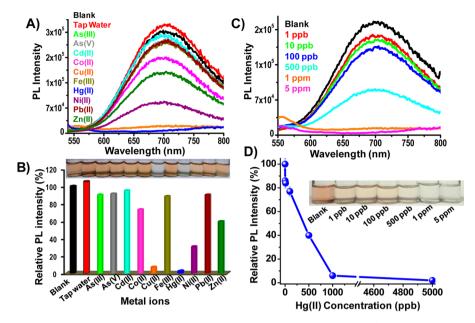

Figure 7. Computed optical spectrum of $Ag_{11}(SCH_3)_7$, structure **f**. The individual optical lines are broadened with 0.05 eV gaussians. The structure is shown as an inset.

at 393, 437, and 487 nm (Figure 1). This structural isomer is within 0.2 eV from the lowest-energy structure. Use of a different (simple, noncharged) thiol in the computational models may explain the uncertainty to assign a prominent "best" structural candidate in this case. Use of the actual glutathione as a ligand would increase the computational effort significantly due to requirements to consider ligand-charging and solvent interactions as well. We also searched structures based on the crystallographically known $Au_{11}(PR_7)Cl_3$ cluster.[44] The resulting cluster is a very high-energy isomer (1.65 eV) and its HOMO−LUMO gap is rather small (0.84 eV) indicating that structural motifs that are known for gold may not be formed for silver.

Clusters for Metal Ion Sensing. The as-synthesized clusters are red luminescent under UV light. This property was utilized for sensing metal ions. A series of transition metal ions, namely, As(III), As(V), Cd(II), Co(III), Cu(II), Fe(III), Hg(II), Pb(II), and Zn(II) were used for this study. Among them, Cu(II) and Hg(II) showed significant quenching in luminescence as shown in Figure 8A. Relative luminescence intensity is plotted in Figure 8B. Corresponding photographs are shown in the inset. Hg(II) contamination in water is one of the examples of heavy metal toxicity. It is known that Hg(II) interacts with the metal cluster core and oxidize the metal, and by this redox process, the luminescence is quenched.[16] We examined the detection limit of Hg(II) using fluorescence intensity. Just after the addition of 1 ppb (final concentration), there is an instant decrease of 15% in the fluorescence intensity. There was a linear decrease with subsequent increase in Hg(II)

Figure 8. (A) Sensitivity of the photoluminescence of $Ag_{11}(SG)_7$ cluster toward different metal ions (5 ppm, final metal ion concentration). The photoluminescence was totally quenched in the presence of Cu(II) and Hg(II). (B) Bar diagram representing the relative decrease in fluorescence intensity in the presence of different metal ions where Hg(II) is showing maximum quenching. Photographs of the samples are shown in the inset. (C) Hg(II) concentration-dependent quenching of cluster luminescence. (D) Relative luminescence intensity vs Hg(II) concentration is plotted showing a linear decrease in emission intensity in the 10−1000 ppb range. Photographs of the corresponding samples are shown in the inset.

concentration up to 1000 ppb, as shown in Figure 8C,D. The detection limit was found to be 1 ppb based on photoluminescence quenching. This is below the limit (2 ppb) set by United States Environmental Protection Agency (US EPA) for drinking water. However, for a practical application, significant additional work is needed. The cluster was sensitive to copper also down to 0.5 ppm due to metallophilic interactions.

SUMMARY AND CONCLUSIONS

In summary, we present a combined experimental and theoretical study of a new silver cluster with molecular formula, $Ag_{11}(SG)_7$. One-step, high yield synthesis resulted in a monodisperse red-luminescent cluster. Theoretical modeling on the structure and UV−vis absorption spectrum support our experimental findings and the formula of the cluster. DFT calculations suggest a seven atom core protected with two $Ag(SR)_2$ and one $Ag_2(SR)_3$ motifs. Detailed mass spectrometric investigation confirmed the presence of a single cluster. Extensive MS/MS was performed to understand the fragmentation pattern and thiolate formation under collision induced dissociation process. Gas phase association of smaller fragments to create larger analogues opens up new possibilities of catalysis, and studies proved the availability of free Ag sites on the cluster fragments, which could yield specific reactions. Finally, Ag_{11} clusters were used in specific sensing of Cu(II) and H(II) ions down to permissible limits in drinking water.

ASSOCIATED CONTENT

Ⓢ Supporting Information

TEM, FTIR, collision energy-dependent ESI MS/MS, computational methods, calculated low energy isomers, and corresponding absorption profiles. This material is available free of charge via the Internet at http://pubs.acs.org.

AUTHOR INFORMATION

Corresponding Author
*(T.P.) E-mail: pradeep@iitm.ac.in. Fax: +91-44-2257-0545.
Author Contributions
§A.B. and M.S.B. contributed equally to this work.
Notes
The authors declare no competing financial interest.

REFERENCES

(1) Jin, R. Quantum Sized, Thiolate-Protected Gold Nanoclusters. *Nanoscale* **2010**, *2*, 343−362.
(2) Wilcoxon, J. P.; Abrams, B. L. Synthesis, Structure and Properties of Metal Nanoclusters. *Chem. Soc. Rev.* **2006**, *35*, 1162−1194.
(3) Parker, J. F.; Fields-Zinna, C. A.; Murray, R. W. The Story of a Monodisperse Gold Nanoparticle: Au25L18. *Acc. Chem. Res.* **2010**, *43*, 1289−1296.
(4) Walter, M.; Akola, J.; Lopez-Acevedo, O.; Jadzinsky, P. D.; Calero, G.; Ackerson, C. J.; Whetten, R. L.; Gronbeck, H.; Hakkinen, H. A Unified View of Ligand-Protected Gold Clusters As Superatom Complexes. *Proc. Natl. Acad. Sci. U.S.A.* **2008**, *105*, 9157−9162.
(5) Udayabhaskararao, T.; Pradeep, T. New Protocols for the Synthesis of Stable Ag and Au Nanocluster Molecules. *J. Phys. Chem. Lett.* **2013**, *4*, 1553−1564.
(6) Diez, I.; Ras, R. H. A. Fluorescent Silver Nanoclusters. *Nanoscale* **2011**, *3*, 1963−1970.
(7) Wei, W.; Lu, Y.; Chen, W.; Chen, S. One-Pot Synthesis, Photoluminescence, and Electrocatalytic Properties of Subnanometer-Sized Copper Clusters. *J. Am. Chem. Soc.* **2011**, *133*, 2060−2063.

21727

dx.doi.org/10.1021/jp508124b | *J. Phys. Chem. C* 2014, 118, 21722−21729

(8) Yuan, X.; Luo, Z.; Zhang, Q.; Zhang, X.; Zheng, Y.; Lee, J. Y.; Xie, J. Synthesis of Highly Fluorescent Metal (Ag, Au, Pt, and Cu) Nanoclusters by Electrostatically Induced Reversible Phase Transfer. ACS Nano 2011, 5, 8800−8808.

(9) Zhang, J.; Wang, X.; Fu, Y.; Han, Y.; Cheng, J.; Zhang, Y.; Li, W. Highly Active Subnano Palladium Clusters Embedded in i-Motif DNA. Langmuir 2013, 29, 14345−14350.

(10) Adhikari, B.; Banerjee, A. Facile Synthesis of Water-Soluble Fluorescent Silver Nanoclusters and HgII Sensing. Chem. Mater. 2010, 22, 4364−4371.

(11) Negishi, Y.; Arai, R.; Niihori, Y.; Tsukuda, T. Isolation and Structural Characterization of Magic Silver Clusters Protected by 4-(tert-Butyl)benzyl Mercaptan. Chem. Commun. 2011, 47 (20), 5693−5695.

(12) Udaya Bhaskara Rao, T.; Pradeep, T. Luminescent Ag_7 and Ag_8 Clusters by Interfacial Synthesis. Angew. Chem., Int. Ed. 2010, 49, 3925−3929.

(13) Krishnadas, K. R.; Udayabhaskararao, T.; Choudhury, S.; Goswami, N.; Pal, S. K.; Pradeep, T. Luminescent AgAu Alloy Clusters Derived from Ag Nanoparticles: Manifestations of Tunable AuI-CuI Metallophilic Interactions. Eur. J. Inorg. Chem. 2014, 2014, 908−916.

(14) Liu, S.; Lu, F.; Zhu, J.-J. Highly Fluorescent Ag Nanoclusters: Microwave-Assisted Green Synthesis and Cr^{3+} Sensing. Chem. Commun. 2011, 47, 2661−2663.

(15) Yu, Y.; Chen, X.; Yao, Q.; Yu, Y.; Yan, N.; Xie, J. Scalable and Precise Synthesis of Thiolated $Au_{10−12}$, Au_{15}, Au_{18}, and Au_{25} Nanoclusters via pH Controlled CO Reduction. Chem. Mater. 2013, 25, 946−952.

(16) Bootharaju, M. S.; Pradeep, T. Facile and Rapid Synthesis of a Dithiol-Protected Ag_7 Quantum Cluster for Selective Adsorption of Cationic Dyes. Langmuir 2013, 29, 8125−8132.

(17) Rao, T. U. B.; Nataraju, B.; Pradeep, T. Ag_9 Quantum Cluster through a Solid-State Route. J. Am. Chem. Soc. 2010, 132, 16304−16307.

(18) Chakraborty, I.; Govindarajan, A.; Erusappan, J.; Ghosh, A.; Pradeep, T.; Yoon, B.; Whetten, R. L.; Landman, U. The Superstable 25 kDa Monolayer Protected Silver Nanoparticle: Measurements and Interpretation as an Icosahedral $Ag_{152}(SCH_2CH_2Ph)_{60}$ Cluster. Nano Lett. 2012, 12, 5861−5866.

(19) Zhou, T.; Rong, M.; Cai, Z.; Yang, C. J.; Chen, X. Sonochemical Synthesis of Highly Fluorescent Glutathione-Stabilized Ag Nanoclusters and S2-Sensing. Nanoscale 2012, 4, 4103−4106.

(20) Chakraborty, I.; Udayabhaskararao, T.; Deepesh, G. K.; Pradeep, T. Sunlight Mediated Synthesis and Antibacterial Properties of Monolayer Protected Silver Clusters. J. Mater. Chem. B 2013, 1, 4059−4064.

(21) Xavier, P. L.; Chaudhari, K.; Baksi, A.; Pradeep, T. Protein-Protected Luminescent Noble Metal Quantum Clusters: an Emerging Trend in Atomic Cluster Nanoscience. Nano Rev. 2012, 3, 14767.

(22) Chakraborty, I.; Udayabhaskararao, T.; Pradeep, T. Luminescent Sub-Nanometer Clusters for Metal Ion Sensing: a New Direction in Nanosensors. J. Hazard. Mater. 2012, 211−212, 396−403.

(23) Zhu, M.; Aikens, C. M.; Hollander, F. J.; Schatz, G. C.; Jin, R. Correlating the Crystal Structure of a Thiol-Protected Au_{25} Cluster and Optical Properties. J. Am. Chem. Soc. 2008, 130, 5883−5885.

(24) Heaven, M. W.; Dass, A.; White, P. S.; Holt, K. M.; Murray, R. W. Crystal Structure of the Gold Nanoparticle $[N(C_8H_{17})_4]$-$[Au_{25}(SCH_2CH_2Ph)_{18}]$. J. Am. Chem. Soc. 2008, 130, 3754−3755.

(25) Zeng, C.; Qian, H.; Li, T.; Li, G.; Rosi, N. L.; Yoon, B.; Barnett, R. N.; Whetten, R. L.; Landman, U.; Jin, R. Total Structure and Electronic Properties of the Gold Nanocrystal $Au_{36}(SR)_{24}$. Angew. Chem., Int. Ed. 2012, 51, 13114−13118.

(26) Qian, H.; Eckenhoff, W. T.; Zhu, Y.; Pintauer, T.; Jin, R. Total Structure Determination of Thiolate-Protected Au38 Nanoparticles. J. Am. Chem. Soc. 2010, 132, 8280−8281.

(27) Jadzinsky, P. D.; Calero, G.; Ackerson, C. J.; Bushnell, D. A.; Kornberg, R. D. Structure of a Thiol Monolayer-Protected Gold Nanoparticle at 1.1 Å Resolution. Science 2007, 318, 430−433.

(28) Crasto, D.; Malola, S.; Brosofsky, G.; Dass, A.; Hakkinen, H. Single Crystal XRD Structure and Theoretical Analysis of the Chiral $Au_{30}S(S-t-Bu)_{18}$ Cluster. J. Am. Chem. Soc. 2014, 136, 5000−5005.

(29) Yang, H.; Lei, J.; Wu, B.; Wang, Y.; Zhou, M.; Xia, A.; Zheng, L.; Zheng, N. Crystal Structure of a Luminescent Thiolated Ag Nanocluster with an Octahedral Ag_{64}^+ Core. Chem. Commun. 2013, 49, 300−302.

(30) Yang, H.; Wang, Y.; Zheng, N. Stabilizing Subnanometer Ag(0) Nanoclusters by Thiolate and Diphosphine Ligands and Their Crystal Structures. Nanoscale 2013, 5, 2674−2677.

(31) Yang, H.; Wang, Y.; Huang, H.; Gell, L.; Lehtovaara, L.; Malola, S.; Häkkinen, H.; Zheng, N. All-Thiol-Stabilized Ag_{44} and $Au_{12}Ag_{32}$ Nanoparticles with Single-Crystal Structures. Nat. Commun. 2013, 4, 2422.

(32) Desireddy, A.; Conn, B. E.; Guo, J.; Yoon, B.; Barnett, R. N.; Monahan, B. M.; Kirschbaum, K.; Griffith, W. P.; Whetten, R. L.; Landman, U.; Bigioni, T. P. Ultrastable Silver Nanoparticles. Nature 2013, 501, 399−402.

(33) Knoppe, S.; Dharmaratne, A. C.; Schreiner, E.; Dass, A.; Burgi, T. Ligand Exchange Reactions on Au_{38} and Au_{40} Clusters: A Combined Circular Dichroism and Mass Spectrometry Study. J. Am. Chem. Soc. 2010, 132, 16783−16789.

(34) Angel, L. A.; Majors, L. T.; Dharmaratne, A. C.; Dass, A. Ion Mobility Mass Spectrometry of $Au_{25}(SCH_2CH_2Ph)_{18}$ Nanoclusters. ACS Nano 2010, 4, 4691−4700.

(35) Hassinen, J.; Pulkkinen, P.; Kalenius, E.; Pradeep, T.; Tenhu, H.; Hakkinen, H.; Ras, R. H. A. Mixed-Monolayer-Protected Au_{25} Clusters with Bulky Calix[4]arene Functionalities. J. Phys. Chem. Lett. 2014, 5, 585−589.

(36) Mathew, A.; Natarajan, G.; Lehtovaara, L.; Hakkinen, H.; Kumar, R. M.; Subramanian, V.; Jaleel, A.; Pradeep, T. Supramolecular Functionalization and Concomitant Enhancement in Properties of Au_{25} Clusters. ACS Nano 2014, 8, 139−152.

(37) Negishi, Y.; Nobusada, K.; Tsukuda, T. Glutathione-Protected Gold Clusters Revisited: Bridging the Gap between Gold(I)-Thiolate Complexes and Thiolate-Protected Gold Nanocrystals. J. Am. Chem. Soc. 2005, 127, 5261−5270.

(38) Niihori, Y.; Matsuzaki, M.; Pradeep, T.; Negishi, Y. Separation of Precise Compositions of Noble Metal Clusters Protected with Mixed Ligands. J. Am. Chem. Soc. 2013, 135, 4946−4949.

(39) Wu, Z.; Lanni, E.; Chen, W.; Bier, M. E.; Ly, D.; Jin, R. High Yield, Large Scale Synthesis of Thiolate-Protected Ag_7 Clusters. J. Am. Chem. Soc. 2009, 131, 16672−16674.

(40) Yuan, X.; Setyawati, M. I.; Tan, A. S.; Ong, C. N.; Leong, D. T.; Xie, J. Highly Luminescent Silver Nanoclusters with Tunable Emissions: Cyclic Reduction-Decomposition Synthesis and Antimicrobial Properties. NPG Asia Mater. 2013, 5, e39.

(41) Bertorelle, F.; Hamouda, R.; Rayane, D.; Broyer, M.; Antoine, R.; Dugourd, P.; Gell, L.; Kulesza, A.; Mitric, R.; Bonacic-Koutecky, V. Synthesis, Characterization and Optical Properties of Low Nuclearity Liganded Silver Clusters: $Ag_{31}(SG)_{19}$ and $Ag_{15}(SG)_{11}$. Nanoscale 2013, 5, 5637−5643.

(42) Udayabhaskararao, T.; Bootharaju, M. S.; Pradeep, T. Thiolate-Protected Ag32 Clusters: Mass Spectral Studies of Composition and Insights into the Ag-Thiolate Structure from NMR. Nanoscale 2013, 5, 9404−9411.

(43) Harkness, K. M.; Tang, Y.; Dass, A.; Pan, J.; Kothalawala, N.; Reddy, V. J.; Cliffel, D. E.; Demeler, B.; Stellacci, F.; Bakr, O. M.; McLean, J. A. $Ag_{44}(SR)_{30}^{4−}$: A Silver-Thiolate Superatom Complex. Nanoscale 2012, 4, 4269−4274.

(44) Abdul Halim, L. G.; Ashraf, S.; Katsiev, K.; Kirmani, A. R.; Kothalawala, N.; Anjum, D. H.; Abbas, S.; Amassian, A.; Stellacci, F.; Dass, A.; Hussain, I.; Bakr, O. M. A Scalable Synthesis of Highly Stable and Water Dispersible $Ag_{44}(SR)_{30}$ Nanoclusters. J. Mater. Chem. A 2013, 1, 10148−10154.

(45) Chakraborty, I.; Udayabhaskararao, T.; Pradeep, T. High Temperature Nucleation and Growth of Glutathione Protected [Similar]Ag75 Clusters. Chem. Commun. 2012, 48, 6788−6790.

(46) Mathew, A.; Pradeep, T. Noble Metal Clusters: Applications in Energy, Environment, and Biology. *Part. Part. Syst. Charact.* **2014**, n/a−n/a.

(47) Habeeb Muhammed, M. A.; Verma, P. K.; Pal, S. K.; Retnakumari, A.; Koyakutty, M.; Nair, S.; Pradeep, T. Luminescent Quantum Clusters of Gold in Bulk by Albumin-Induced Core Etching of Nanoparticles: Metal Ion Sensing, Metal-Enhanced Luminescence, and Biolabeling. *Chem.—Eur. J.* **2010**, *16*, 10103−10112.

(48) Liu, Y.; Ai, K.; Cheng, X.; Huo, L.; Lu, L. Gold-Nanocluster-Based Fluorescent Sensors for Highly Sensitive and Selective Detection of Cyanide in Water. *Adv. Funct. Mater.* **2010**, *20*, 951−956.

(49) Kumar, S.; Bolan, M. D.; Bigioni, T. P. Glutathione-Stabilized Magic-Number Silver Cluster Compounds. *J. Am. Chem. Soc.* **2010**, *132*, 13141−13143.

(50) Bellon, P.; Manassero, M.; Sansoni, M. Crystal and Molecular Structure of Triiodoheptakis[tris(*p*-fluorophenyl)phosphine]-undecagold. *J. Chem. Soc., Dalton Trans.* **1972**, *14*, 1481−7.

(51) Bernhardt, T. M.; Hagen, J.; Lang, S. M.; Popolan, D. M.; Socaciu-Siebert, L. D.; Woste, L. Binding Energies of O_2 and CO to Small Gold, Silver, and Binary Silver-Gold Cluster Anions from Temperature Dependent Reaction Kinetics Measurements. *J. Phys. Chem. A* **2009**, *113*, 2724−2733.

(52) De, H. J.; Veldeman, N.; Claes, P.; Janssens, E.; Andersson, M.; Lievens, P. Carbon Monoxide Adsorption on Silver Doped Gold Clusters. *J. Phys. Chem. A* **2011**, *115*, 2103−2109.

(53) Popolan, D. M.; Noessler, M.; Mitric, R.; Bernhardt, T. M.; Bonacic-Koutecky, V. Composition Dependent Adsorption of Multiple CO Molecules on Binary Silver-Gold Clusters $Ag_nAu_m^+$ ($n + m = 5$): Theory and Experiment. *Phys. Chem. Chem. Phys.* **2011**, *12*, 7865−7873.

(54) Nie, X.; Qian, H.; Ge, Q.; Xu, H.; Jin, R. CO Oxidation Catalyzed by Oxide-Supported $Au_{25}(SR)_{18}$ Nanoclusters and Identification of Perimeter Sites as Active Centers. *ACS Nano* **2012**, *6*, 6014−6022.

(55) Nie, X.; Zeng, C.; Ma, X.; Qian, H.; Ge, Q.; Xu, H.; Jin, R. CeO_2-Supported $Au_{38}(SR)_{24}$ Nanocluster Catalysts for CO Oxidation: a Comparison of Ligand-on and -off Catalysts. *Nanoscale* **2013**, *5*, 5912−5918.

(56) Wu, Z.; Jiang, D.-E.; Mann, A. K. P.; Mullins, D. R.; Qiao, Z.-A.; Allard, L. F.; Zeng, C.; Jin, R.; Overbury, S. H. Thiolate Ligands as a Double-Edged Sword for CO Oxidation on CeO_2 Supported $Au_{25}(SCH_2CH_2Ph)_{18}$ Nanoclusters. *J. Am. Chem. Soc.* **2014**, *136*, 6111−6122.

21729

dx.doi.org/10.1021/jp508124b | *J. Phys. Chem. C* 2014, 118, 21722−21729